Monolithic Integration of an Electroabsorption Modulator into a GaAs-based Duo-cavity VCSEL for Resonance-free Modulation

J. van Eisden[1], M. Yakimov[1], V. Tokranov[1], E. M. Mohammed[2], I. A. Young[2] and S. R. Oktyabrsky[1]

[1]*College of Nanoscale Science and Engineering, SUNY Albany, Albany, NY*
Tel.:(518)-437-8609, email:myakimov@uamail.albany.edu
[2]*Intel Corporation, Hillsboro OR*

Keywords: Vertical cavity Surface Emitting Laser (VCSEL), High-frequency modulation, Semiconductor lasers, Fabri-Perot Cavities

Abstract

A novel device concept of Vertical Cavity Surface Emitting Laser (VCSEL) with integrated modulator is demonstrated. Gain and absorption media are positioned in two Fabri-Perot cavities formed by three DBR stacks. Tuning relative spectral positions of two cavities resonances allows operation without optoelectronic feedback, extending modulation response well beyond optoelectronic resonance frequency.

INTRODUCTION

Optoelectronic resonance effect imposes a fundamental limitation on maximum direct modulation frequency of semiconductor lasers [1]. A commonly used, but relatively expensive approach includes using an external modulator with optical isolators to achieve high modulation bandwidth. Electro-optical modulator can be integrated directly into the laser cavity, however optical feedback still limits high frequency modulation characteristics of the device due to parasitic optical feedback.

We propose an alternative solution, which allows using a modulator, monolithically integrated with VCSEL without optical feedback to achieve high modulation frequencies.

DEVICE STRUCTURE

Overall structure of device is similar to a regular VCSEL, with a second Fabri-Perot cavity being used as a top low-reflectivity mirror (FP mirror, as shown in Fig.1).

A calculated reflection and transmission spectra of such FP mirror, consisting of two DBRs with controllable absorber in between is shown in Fig.2. Spectra for three different values of absorption– 0, 0.5% and 1% per round-trip - are calculated using a 1-D transfer matrix model. It can be seen that the reflectivity remains independent of absorption at certain wavelengths on both blue and red side of the resonance. Also, there is a clear change in transmission at different absorptions at those wavelengths. By using such a cavity as a top mirror of a regular VCSEL structure and aligning the VCSEL wavelength to one of the zero-*DR* cross-over spots, the VCSEL output can be modulated while keeping the reflectivity constant as seen by the gain medium. As a result, we can expect that both optical field and carrier concentration in the gain section would remain independent of modulation signal, thus avoiding limitations imposed by optoelectronic resonance. The most apparent drawbacks of such design are limited modulation depth and tight requirements for spectral alignment of two cavities.

The limitation on modulation power depth comes from the fact that transparency of the FP mirror has limited variability, as can be seen in Fig. 2.

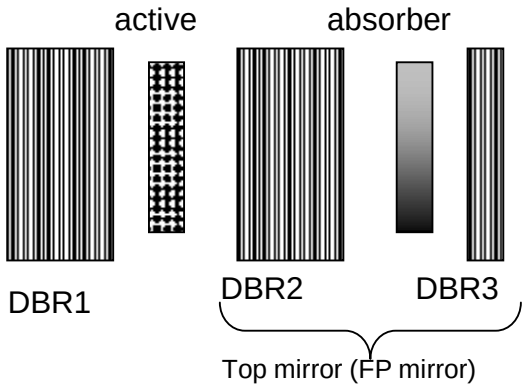

Fig. 1. Schematic diagram of integrated VCSEL-modulator device. Second Fabri-Perot cavity is used as a top mirror. Spectra of such a FP mirror is shown in fig. 2

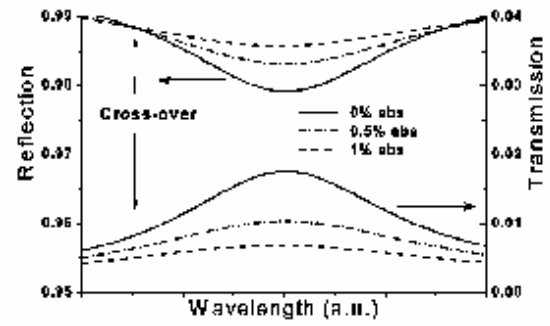

Fig. 2 Calculated reflection and transmission spectra of a Fabri-Perot cavity with variable intracavity absorption showing one of two cross-over wavelengths where reflectivity is independent of absorption

Devices were grown in a single epitaxial run using an EPI Gen II Molecular Beam Epitaxy (MBE) system. In growth order, device structure consists of

- bottom Distributive Bragg Reflector (DBR) with 29 periods of n-type $Al_{0.07}Ga_{0.93}As$ / $Al_{0.90}Ga_{0.10}As$ λ/4 layers,
- an active region with a n^{++}-p^{++} tunneling junction and a set of four quantum wells (QW) with p-type modulation doping
- 32 periods of n-doped middle DBR,
- an approximately λ or 1½ λ thick modulator section with absorber embedded in the i-region of p-i-n junction. We used five split QWs to create a voltage-controlled absorber [3]
- and 9 periods of p-type top DBR.

n^{++}-p^{++} tunneling junction was incorporated directly under the active region so that both middle and bottom DBRs are n-doped in order to reduce optical losses in the device induced by higher free-carrier absorption of p-doped AlGaAs close to the active region. Fine tuning of the resonances is done by changing the thickness of the modulator diode section slightly different from the half-wavelength integer.

Two parts of the device - gain section and absorber – are independently driven through three device terminals (see Figure 3):

- a backside n-type contact shared by all the devices on a wafer,
- an intracavity n-type contact to the middle DBR, which is common terminal to both diode sections and an RF ground,
- and a top p-type contact.

The active region of the laser is driven by a DC current, while both RF signal and DC bias can be applied to the modulator junction. Current apertures for the device are created by ion implantation for the modulator, and by wet lateral oxidation combined with field implantation for the active region.

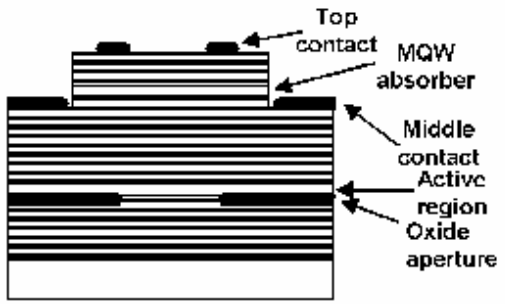

Fig. 3 Schematic diagram of the device layout, showing two device sections (active region and absorber) and contacts locations

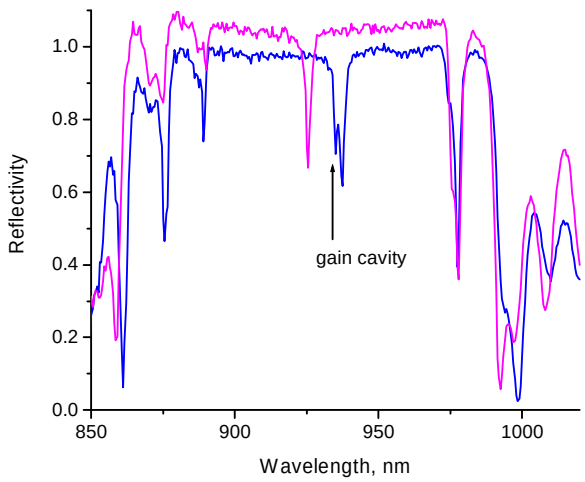

Fig. 4. Top-down reflectivity spectrum of an as-grown device wafer, showing spectra of optically aligned (blue) and misaligned (purple, offset by 0.05 for clarity) structure. Position of the gain cavity is the same in both cases

RESULTS

Figure 4 shows the top-down reflectivity spectrum of an as-grown device wafer with detuning between the two resonances. The active region resonance is visible on the red side shoulder of the modulator section resonance.

Typical modulation responses for direct modulated VCSEL, VCSEL with electro-absorption modulator integrated into the cavity and duo-cavity device are shown on fig. 5.

20 db/decade roll-off above 5 GHz is due to RC parasitics, primarily capacitance of metallization and capacitance of reverse biased p-i-n modulator diode are present for all three devices. An ω^{-2} roll-off due to optoelectronic resonance in addition to RC roll-off results a 60 db/decade slope for a directly modulated device. A ω^{-1} roll-off for a VCSEL with intracavity modulator was previously described [3] and demonstrated [4]. However, improved high frequency response comes at a cost of much stronger resonance and modulation response being non-linear at those frequencies. The duo-cavity device does not demonstrate any response-limiting features other than RC.

Capacitance issues were addresses in a second-pass devices with redesigned metallization and improved modulator i-region design. Fabricated devices have shown flat high frequency responses within +/- 3 dB up to 19 GHz, with a single high-frequency roll-off pole still entirely determined by the metallization and modulator section parasitics (see Figure 6) as determined by S-parameter analysis and fitting to electrical equivalent circuits. Engineering of the modulator section has been done by adjusting cavity thickness to reduce diode junction capacitance, and absorber MQW configuration in order to

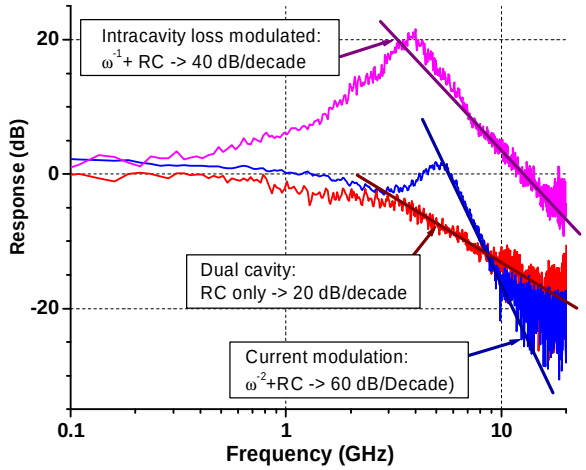

Fig. 5. Modulation response for a direct current modulated, intracavity loss modulated, and dual cavity devices. 20 db/decade roll-off above 5 GHz is due to RC parasitic it metallization

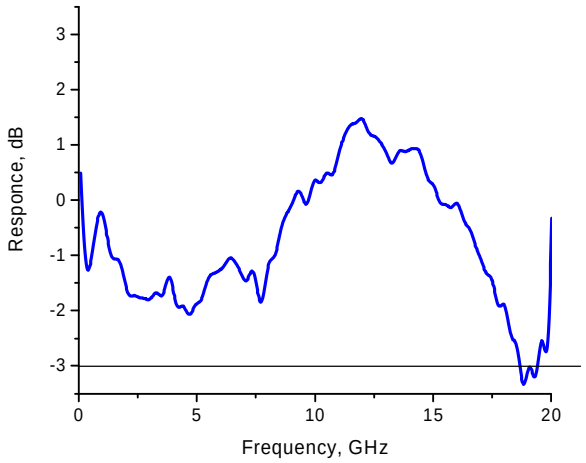

Fig.6. Device high frequency modulation response at room temperature. Drive current 7mA, modulator bias 0.4 V..

obtain a greater modulation depth. The obtained modulation depth is ~40% at an output power of 1.2 mW, as shown on light-power characteristic in fig. 7.

Further proof of cavities decoupling concept can be done by varying optical of the cavities while monitoring modulation response. This can be done through variation of voltage applied to the modulator section: such variation results in change of both imaginary and real part of refraction index, thus changing not only absorption within second cavity, but also optical alignment of the cavities.

Data presented in Fig. 8 demonstrates different types of modulation curves, which can be obtained from a single device. At -0.4V both cavities are close to desired alignment, resulting in almost flat optical response; at -0.1V cavities are misaligned, so a resonance peak around 10 GHz is clearly visible.

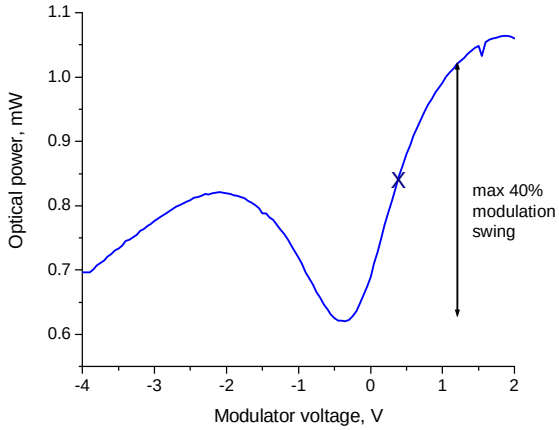

Fig. 7 Light power dependence on modulator voltage for a dual cavity device, showing 40% modulation. Frequency response in fig. 6 is taken at a point marked by "X"

The most interesting behavior is observed at +0.4V with resonance response being suppressed rather than increased. In order to understand that, lets consider factors affecting light output:

Output light power of device with variable mirror transparency is proportional to mirror transparency T and photon concentration inside the cavity N_p:

$$I_{out} \sim N_p * T.$$

In case non-ideal alignment of optical cavities both reflection and transmission of FP mirror vary, resulting in modulating both N_p and T:

$$\Delta I_{out} \sim \Delta(N_p * T) = N_p * \Delta T + \Delta N_p * T,$$

where first term describes purely decoupled behavior, while the second term describes modulation of output power due to optical feedback of the active medium.

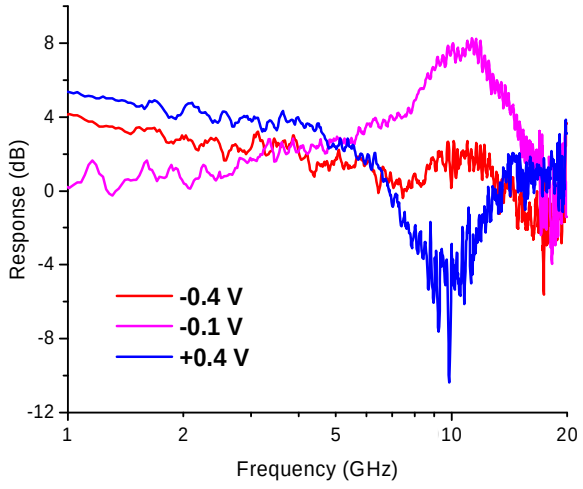

Fig. 8 Modulation response of a dual-cavity devices at different modulator voltages. Change of modulator voltage causes shift of optical cavity position, thus detuning from ideal situation (red curve). Detuning may result in optical feedback-related modulation being in-phase (purple) or 180^0 shifted (blue) with decoupled mode modulation

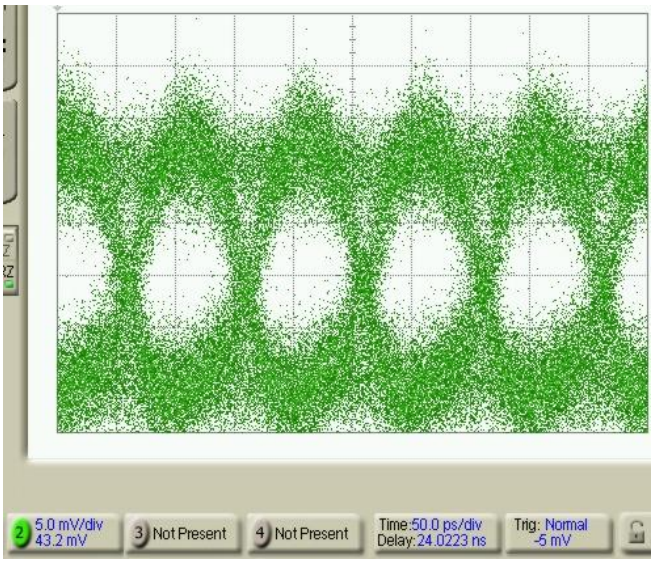

Fig. 9. A 10 Gbit/s eye diagram of dual cavity device showing an open eye.

In case one of these terms dominates, modulation response can be either a mostly flat or feature a strong resonance with high-frequency roll-off. However, when absolute values of both terms are close a more complicated shape of response curve can be observed.

From Fig. 2 it can be seen that mirror reflectivity can either increase or decrease with increased absorption, resulting in either in-phase or 180^0 phase shifted optical feedback depending on relative alignment of the cavities. Adding in-phase or phase-shifted component to a flat response can result in either amplified or suppressed resonant frequency response, with both of these situations shown in fig. 8.

A 10 Gbit/s eye diagram of a dual cavity device is presented in fig. 9. A 7.5 GHz low-pass filter was used to reduce effect of high-frequency device noise.

CONCLUSIONS

We have developed a monolithically integrated duo-cavity VCSEL-Modulator device capable of high-frequency operation without optoelectronic resonances. In the intended configuration the intrinsic modulation bandwidth limit is determined by metallization and modulator junction parasitics only. A flat (+/- 3 dB) modulation response up to 19 GHz has been shown.

ACKNOWLEDGEMENTS

This work has been funded by Intel corporation, the SRC and NSF project number ECCS S0725523 and Interconnect Focus Center program.

REFERENCES.

1. L. Coldren, S. Corzine. (1995*) Diode lasers and Photonic Integrated Circuit.* NewYork: John Wiley & sons, inc.
2. N.Debbar, S. Hong, J. Singh, P. Bhattacharya, R. Sahai, “Coupled GaAs/AlGaAs quantum-well electroabsorption modulators forlow-electric-field optical modulation” Journ. of Appl. Phys., **65**, 383, (1989)
3. E. A. Avrutin, V. B. Gorfinkel, S. Luryi and K. A. Shore “Control of surface-emitting laser diodes by modulating the distributed Bragg-mirror reflectivity: Small-signal analysis” Appl. Phys. Lett,**63**, 18,(1993)
4. J. van Eisden et al. ”Modulation Properties of VCSEL with intracavity Modulator” Proc. SPIE Int. Soc. Opt. Eng. 6484, 64840A (2007)

ACRONYMS

VCSEL: vertical Cavity Surface Emitting Laser
DBR: Distributed Bragg Reflector
QW: Quantum Well
FP mirror: Fabri-Perot mirror (Fabric-Perot cavity is used as a mirror for the laser)